

AperTO - Archivio Istituzionale Open Access dell'Università di Torino

Chemical inhibition of xylem cellular activity impedes the removal of drought-induced embolisms in poplar stems - new insights from micro-CT analysis

This is a pre print version of the following article:

Original Citation:

Availability:

This version is available <http://hdl.handle.net/2318/1765649> since 2021-10-22T13:27:45Z

Published version:

DOI:10.1111/nph.16912

Terms of use:

Open Access

Anyone can freely access the full text of works made available as "Open Access". Works made available under a Creative Commons license can be used according to the terms and conditions of said license. Use of all other works requires consent of the right holder (author or publisher) if not exempted from copyright protection by the applicable law.

(Article begins on next page)

X-ray micro CT analyses of embolism formation and impact of cellular activity on xylem recovery from stress in poplar trees

Francesca Secchi¹, Chiara Pagliarani², Silvia Cavalletto¹, Francesco Petruzzellis³, Giulia Tonel¹, Tadeia Savi³, Giuliana Tromba⁴, Maria Margherita Obertino¹, Claudio Lovisolo¹, Andrea Nardini³, Maciej A. Zwieniecki⁵

¹) Department of Agriculture, Forest and Food Sciences, University of Turin, Largo Paolo Braccini 2, 10095 Grugliasco, Italy

²) Institute for Sustainable Plant Protection, National Research Council, Strada delle Cacce 73, Torino, Italy

³) Dipartimento di Scienze della Vita, University of Trieste, via Giorgieri 10, 34127 Trieste (Italy)

⁴) Elettra-Sincrotrone Trieste, Area Science Park, 34149 Basovizza, Trieste, Italy

⁵) Department of Plant Sciences, University of California Davis, One Shields Avenue, 95616 Davis (CA), USA

Author for correspondence:

Francesca Secchi

Tel: +39 011 6708655

Email: francesca.secchi@unito.it

Total word count (excluding summary, references and legends):		No. of figures:	6
Summary:		No of Tables:	0
Introduction:		No. of Supporting Information files:	1 (Fig. S1)
Material and Methods:			
Results:			
Discussion and Conclusion:			
Acknowledgements			

Summary

In drought stressed plants a coordinated cascade of chemical and transcriptional adjustments occurs concurrently to embolism formation. While these processes do not affect embolism formation during stress, they may prime stems for recovery during rehydration by modifying apoplast pH and increasing sugar concentration in the xylem sap.

Here we show that *in vivo* treatments modifying apoplastic pH (stem infiltration with a pH buffer) or reducing stem metabolic activity (infiltration with sodium vanadate and sodium cyanide; plant exposure to carbon monoxide) can reduce sugar accumulation, thus disrupting or delaying the recovery process.

Application of the vanadate treatment (NaVO_3 , an inhibitor of many ATP-ases) completely halted recovery from drought-induced embolism for up to 24 hours after re-irrigation, while partial recovery was observed *in vivo* in control plants using X-ray micro-CT.

Our results suggest that stem hydraulic recovery in poplar is a biological, energy dependent process that coincides with accumulation of sugars in the apoplast during stress. Recovery and damage are spatially coordinated, with embolism formation occurring from the inside-out and refilling from the outside-in. The outside-in pattern highlights the importance of xylem proximity to the sugars within the phloem to the embolism recovery process.

Key words: apoplastic pH, embolism, *Populus*, recovery, sugars, X-ray micro-computed tomography (micro-CT), vanadate, xylem

Introduction

Survival of vascular plants under drought is intimately linked to maintaining the functionality of their xylem network. While physical aspects of long-distance water transport in vascular plants and formation/spread of embolism are well understood (Stroock *et al.*, 2014; Jensen *et al.*, 2016), the biology of active recovery from embolism remains hotly debated (Nardini *et al.*, 2011; Brodersen & McElrone, 2013; Knipfer *et al.*, 2016). Groups of researchers think that, in some species, no embolism recovery occurs under natural conditions (Charrier *et al.*, 2016; Lamarque *et al.*, 2018; Choat *et al.*, 2019) while others assert that recovery is a common process that can take place even under moderate xylem tensions (Salleo *et al.*, 2009; Zwieniecki & Holbrook, 2009; Brodersen *et al.*, 2010; Secchi & Zwieniecki, 2011; Tomasella *et al.*, 2019a). Major controversies originate from the fact that the most of the techniques used to study plant hydraulic properties are destructive, and with doubted reliability (Cochard *et al.*, 2013). Some techniques could indeed cause artefacts (e.g. increased percent loss of conductivity (PLC) values) due to the excision of xylem under tension, thus potentially allowing for spurious air entry into the conduits even if stems were cut under water (Wheeler *et al.*, 2013). Other techniques can cause supersaturation with positive air pressure that could induce embolism and the appearance of its rapid recovery. However, the presence and significance of these artefacts are questioned (Trifilo *et al.*, 2014; Fukuda *et al.*, 2015; Scoffoni & Sack, 2015; Ogasa *et al.*, 2016; Nardini *et al.*, 2017; Nolf *et al.*, 2017).

Classical hydraulic techniques for monitoring the presence of xylem embolism are complemented with *in-vivo*, non-destructive techniques like magnetic resonance imaging (MRI) (Holbrook *et al.*, 2001; Clearwater & Goldstein, 2005; Wang *et al.*, 2013; Zwieniecki *et al.*, 2013) and X-ray computed micro-tomography (X-ray micro-CT; Brodersen *et al.*, 2010; McElrone *et al.*, 2013; Choat *et al.*, 2016). These contemporary techniques make it possible to observe, in real time, the spatial and temporal patterns of embolism occurrence in the hydraulic systems of living plants. The MRI, while very safe for living cells and capable of fast, repetitive imaging, has relatively low resolution ($>20\text{ }\mu\text{m}$) and physical limitations on fitting the stem through the core of the magnet. X-ray micro-CT has emerged as the preferred technique for studying xylem embolism formation (Cochard *et al.*, 2015) and its potential recovery (Brodersen *et al.*, 2010; Rolland *et al.*, 2015; Brodersen *et al.*, 2018). X-ray micro-CT provides good

contrast between air-filled and water-filled conduits, high spatial and temporal resolution (~1 μm) and high signal-to-noise ratio. However, a recent study challenged the usefulness of X-ray micro-CT for repeated observations of water content in the same xylem conduits due to the severe damage caused to living cells by consecutive scans (Petruzzellis *et al.*, 2018). Limiting xylem exposure to single scans, and reliance on observations of multiple stems, might be required to confidently study the hydraulic recovery processes.

Despite these technical difficulties, a growing consensus suggests, that while embolism formation cannot be avoided during severe water stress, recovery might be possible upon relief of stress (lowering tension) and strongly reduced transpiration (Brodersen & McElrone, 2013). To account for this process, several recovery models were proposed (Salleo *et al.*, 2004; Zwieniecki & Holbrook, 2009; Nardini *et al.*, 2011; Brodersen & McElrone, 2013; Secchi & Zwieniecki, 2016; Pagliarani *et al.*, 2019), suggesting that the living parenchyma cells associated with xylem (vascular associated cells - VACs) are directly involved in supplying the water, energy and osmotica needed to repair embolized vessels. During drought, soluble sugar content (mostly sucrose) is proposed to increase in VACs due to elevated starch degradation rates and the necessity of lowering cell osmotic potential in the xylem (Salleo *et al.*, 2009; Secchi & Zwieniecki, 2011; Secchi & Zwieniecki, 2016). Increased sugar levels in VACs trigger sucrose efflux to the apoplast via sucrose transporters. Local levels of sugar might be supplemented by sugars supplied from the phloem, decreasing reliance on locally stored starch (Nardini *et al.*, 2011). Sugars and ions accumulated in the apoplast can generate up to ~ 0.2 MPa osmotic pressure in non-functional vessels (Secchi & Zwieniecki, 2012), and thus build-up an osmotic gradient that allows for cell-by-cell refilling against low tension (Zwieniecki & Holbrook, 2009). *In vivo* observations from both MRI and X-ray micro-CT studies confirm that water may return to empty vessels if a significant reduction in stress occurred (Holbrook *et al.*, 2001; Scheenen *et al.*, 2007; Zwieniecki *et al.*, 2013; Brodersen *et al.*, 2018), and that water droplets preferentially form and grow on the vessel walls that are in contact with VACs (Brodersen *et al.*, 2010).

The efflux of sugars is induced by low apoplastic pH conditions that promote the activity of acidic invertases. In a low pH environment, acidic invertases splice sucrose to glucose and fructose, thus reducing the concentration of extracellular sucrose and generating a sucrose gradient between VACs and the apoplast, promoting further sucrose efflux from parenchyma. Simultaneously, acidic invertase activity results in the accumulation of monosaccharides in

xylem sap, doubling the osmotic potential contributed by sucrose. Active pH adjustment has been confirmed in poplar, where, as predicted by theoretical models, drought induces a pH decrease in the apoplast, causing sugar accumulation in the xylem (Secchi & Zwieniecki, 2016). These stress-related physiological activities are closely coupled to upregulation of gene expressions involved in starch digestion, maltase and sucrose transport and acidic invertases (Pagliarani *et al.*, 2019). All of these observed physiological and transcriptional events are consistent with the priming of xylem for the recovery process. Still required to settle the embolism debate, are *in vivo* observations of xylem embolism and recovery, paired with experimental perturbation of xylem chemistry.

Although successful hydraulic recovery necessitates the activity of living parenchyma cells near the xylem, the direct involvement of VACs in this process has not been demonstrated. To verify VAC involvement, we perturbed stem biological activity while concurrently visualizing the hydraulic recovery process. We hypothesized that, if sap acidification represents a symptom/signal of severe water stress and if pH-driven sugar accumulation primes stems for embolism recovery when stress is relieved, then inhibition of the biological activity of parenchyma cells during stress will limit, or entirely halt, the hydraulic recovery processes. To test this hypothesis, we used X-ray micro-CT observations of poplar stems under stress and post-rehydration in combination with treatments inhibiting the metabolic activity of VACs. Our findings reveal that: a) poplar trees can reduce embolism extent following water stress relief; b) embolism formation and disappearance are spatially coordinated, with embolisms accumulating from the inside-out, and recovery occurring from the outside-in, c) experimental reduction of the metabolic activity of dehydrated plants significantly impedes the removal of drought-induced embolisms.

Material and Methods

Plant material and growth conditions

Four month-old hybrid poplars (*Populus tremula* x *Populus alba* clone 717-1B4) were initially grown in a greenhouse at the University of Turin under partially controlled climatic conditions. The greenhouse air temperature and relative humidity averaged 22°C and 55% respectively. Maximum photosynthetic photon flux density (PPFD) ranged between 1200 and 1400 μmol

photons $\text{m}^{-2} \text{s}^{-1}$ and 12-h-light/12-h-dark cycles were followed using halogen lamps when necessary, to supplement light and guarantee a minimum PPFD of 500-600 $\mu\text{mol photons m}^{-2} \text{s}^{-1}$. Each plant grew in a 2 L pot filled with a substrate composed of sandy-loam soil, expanded clay, and peat (2:1:1 by weight). The experiment was conducted on 67 total poplars, ~50 cm tall with a stem diameter of 3 to 4 mm. One sub-group of poplars (35 plants) was maintained in the greenhouse at University of Turin, these poplars were used for the chemical manipulations and preliminary analysis of xylem sap. This approach allowed us to determine the timeline of each treatment to optimize time-frame selection for direct X-ray micro-CT observations. A second subset of poplars (32 plants) was moved ahead of the *in vivo* experiment to the greenhouse at the University of Trieste to allow three weeks of acclimation prior to the experiments conducted at the Elettra Sincrotrone Trieste facility.

Experimental design

(1) Chemical manipulations (at University of Turin)

35 plants were used in this study. Five plants were kept as controls (*CTR*) and watered every day to field capacity. The remaining 30 plants were gradually subjected to water stress (*WS*) by reducing irrigation until the stem water potential (Ψ_{stem}) was below -1.8 MPa, a value corresponding to at least 50 % of PLC (Secchi & Zwieniecki, 2014). Once the target water-stress level was reached, xylem sap was collected from five plants (*stressed, not treated*); using a destructive method (Secchi & Zwieniecki, 2012), the other five stressed poplars were re-watered and allowed to recover over the period of 24 hours (*recovered, not treated*). After one day of stress relief, xylem sap was collected. Before the re-watering phase, the remaining 20 water stressed poplars were subjected to different chemical manipulations (five plants for each of four treatments) to inhibit the metabolic activity of wood parenchyma cells (Fig. 1a). Four different manipulations were applied:

a) Stem infiltration with distilled water plus sodium orthovanadate (NaVO_3 , BioLabs, New England, MA), a general inhibitor of many plasma membrane proton pumps, expected to reduce changes in apoplastic pH. The vanadate solution was used at a concentration of 10 mM.

b) Stem infiltration with distilled water plus sodium cyanide (NaCN, Sigma), to block respiration and consequently, ATP-ase activity. The NaCN solution was used at a concentration of 1.0 mM.

c) Stem infiltration with pH 6.5 buffer solution (100mL of 0.1 M Potassium dihydrogen phosphate, 27.8 ml of 0.1M Sodium hydroxide, 72.2 ml of distilled water), for directly altering apoplastic pH.

d) whole plant exposure to carbon monoxide (CO) gas, for impairing the oxidative respiration and, consequently, ATP-ase activity.

For stem infiltration, 2-3 fully expanded leaves, at around 1/3 tree height, were cut-off leaving petiole attached to the stem. Then a 2.5 cm-long silicon rubber tubing was attached at the remaining petioles and filled with 200 µl of solution (see Fig. 1b). Solutions were allowed to infiltrate the stem via natural stem suction for two hours. If the absorbed volume exceeded the volume of the solution in the tube, additional liquid was added; on average a total of ~0.75 ml of solution was absorbed into vascular system of each treated plant. Treated plants were allowed 1-day for acclimation, then re-watered and allowed 24 hours of recovery time (*recovered, treated*) before xylem sap collected for chemical analyses.

During the carbon monoxide treatment, poplar trees were placed in transparent plastic bags (Fig. 1c). Bags were initially deflated and later filled with CO applied thorough a silicon tube connected to a CO tank until the plastic bag was fully inflated. For the next 3 hours, the plants were maintained isolated in the CO-filled bags. After bag removal, treated plants were allowed 1 day of acclimation, then re-watered and allowed 24 hours of recovery time (*recovered, treated*) before xylem sap was extracted.

(2) Plant preparation for X-ray micro-CT observation (at University of Trieste)

The part 32 plants used for this part of the study, were further divided into two groups; 16 poplars (OV group) to be treated with a sodium ortho-vanadate solution as described above, while the 16 plants belonging to the control group were left untreated. In each group, 4 plants were kept as unstressed control and watered every day. The remaining 12 plants were subjected to water stress (<-1.8 MPa). After plants reach the target water-stress level, the OV group was treated (as described for Turin experiment). Eight plants from both the control and OV groups were then re-watered. X-ray micro-CT observations were performed on all

control, stressed, and recovered plants (four hours, until 24 hours of recovery time, with only one scan per plant) at Elettra Sincrotrone Trieste, using the SYRMEP beamline (www.elettra.trieste.it), (see below for specifics of X-ray, micro-CT observations)

Measurements of stem water potential

Stem water potential was measured for each plant on equilibrated non-transpiring (bagged) leaves. Mature leaves were covered with aluminum foil and placed in a humidified plastic bag for at least 30 minutes before excision. After excision, leaves were allowed to equilibrate for more than 20 minutes in dark conditions before measuring water potential with a Scholander-type pressure chamber in Turin (Soil Moisture Equipment Corp., Santa Barbara, CA, USA) and with a portable pressure chamber (3005 Plant Water Status Console, Soilmoisture Equipment Corp., Goleta, CA, USA) in Trieste. Stem xylem-pressure changes were monitored for the duration of the experiments, from the beginning of the stress treatment until full recovery with varying frequency days (drying) to hours (recovery).

Sap sampling procedure

Xylem sap from functional vessels was collected from control, stressed, recovered treated and not treated plants (method in Secchi & Zwieniecki, 2012). Sap samples were kept at -20°C until analyses were conducted.

Soluble carbohydrate content and pH measurements

The anthrone-sulfuric acid assay (Leyva *et al.*, 2008) was used to quantify soluble carbohydrate content in xylem sap liquids. The anthrone reagent was prepared immediately before analysis by dissolving 0.1 g of anthrone (0.1%) in 100 mL of concentrated sulfuric acid (98%). Standard solutions were prepared by diluting a Glucose Standard Solution (1.0 mg/ml; Sigma, Saint Louis, Missouri, USA). We added, 150 µl of anthrone reagent to each well of the microplate containing 50 µL of standard solutions, positive control (water), sample solutions, and a blank. Plates were kept for 10 min at 4 °C, then incubated for 20 min at 100 °C. After heating, plates were cooled down for 20 min at room temperature before absorbance at 620 nm was read with a microplate reader (Multiscan Thermo Scientific). Colorimetric response was compared to the glucose

standard curve (0, 0.01, 0.03, 0.1, and 0.3 mg L⁻¹ glucose) and total carbohydrate content was calculated as mg/mL of glucose.

The pH measurements were taken on sap samples using a micro pH electrode (PerpHect® ROSS®, Thermo Fischer Scientific, Waltham, MA USA).

X-ray Micro-CT observations

Potted poplars were transported to the beamline (see above). Prior to X-ray micro-CT observations, stem water potential was measured on each plant. To reduce sample movement during scan rotation, the whole plant was wrapped in plastic film and secured to a wood skewer; the pot was then fixed to the beamline sample holder such that stem distance was 10 cm from the detector. The stem was scanned at about 4 cm above the root collar. Two silicon filters (0.5 mm each) were used to obtain an average X-ray source energy of 25 keV, resulting in an entrance dose rate in water of 47 mGy s⁻¹. X-ray window was 4 mm in height with horizontal opening up to 120 mm. The exposure time was set at 100 ms, at an angular step of 2° resulting in a 3 min-long scan. During the 360° rotation of the sample, a total of 1600 images were acquired (see Petruzzellis *et al.*, 2018). In total 32 plants were scanned and each plant was subjected to only one exposure. After the scan, 14 stems were air-cut a few mm below the scanned section to induce the maximum artificial embolism. Only these samples were then re-scanned and analyzed as the others, providing an additional normalization standard for PLC calculations.

In total, 1600 slices per sample with a spatial resolution of 2 µm were reconstructed using the software SYRMEP TomoProject (Brun *et al.*, 2015) and one micro-CT slice per sample was analyzed with the Image J (1.46r, NIH, <https://imagej.nih.gov>) software. For each sample, the transverse area of all gas-filled (dark grey) and water-filled (light grey) xylem conduits, the total area of xylem and the distance from embolized vessels to cambium were measured.

The average diameter of each conduit (derived from its area, and assuming a circular shape) was used to calculate the theoretical hydraulic conductivity (K_t) of the xylem, using the Hagen-Poiseuille equation (Tyree & Zimmermann, 2002). The sum of gas-filled (K_{t_{gas}}) and water-filled (K_{t_{water}}) vessel conductivities provided total xylem conductivity (K_{t_{max}}). The theoretical PLC was then calculated as (K_{t_{gas}} / K_{t_{max}}) x 100.

Statistical analyses

Significant differences among treatments were tested by one-way analysis of variance (ANOVA). The Fisher LSD post-hoc test was used for separating means when ANOVA results were significant ($P < 0.05$). Pairwise differences between treatment means were compared with Student's t -test. The SPSS statistical software package (v24.0, SPSS Inc., Cary, NC, USA) and Sigma Plot software (Systat software Inc., San Jose, USA) were used to run the statistical analyses reported above and to create figures, respectively.

Results

X-ray micro-CT observations of xylem in intact poplar plants allowed us to distinguish water-filled (functional) and gas-filled (non-functional) vessels (Fig. 2a). Almost all vessels in non-stressed plants (stem water potential in the range of 0 to -0.5 MPa) were water-filled (Fig. 2b-2). Any higher level of stress (water potential < -0.5 MPa) was associated with an increase of gas-filled conduits number (Fig. 2a and 2b-3). The calculated theoretical conductance of water filled vessels vs. the conductance of all vessels was used to generate a vulnerability curve (percent loss of conductivity (PLC) versus xylem pressure) and data were fitted to a four-parameter, dose-response logistic curve (Fig. 2a, grey circles and grey lines). While the shape of the obtained curve was similar to typical PLC curves, maximum PLC for severely stressed plants only reached ~50% (Fig. 2a, red circles), a value lower than that reported previously (Secchi & Zwieniecki, 2014). However, when maximum conductance was determined using only functional vessels (the ones that embolized after cutting in air), the recalculated PLC matched the previous hydraulic measurements (Fig. 2a – black circles and blue lines). When subtracting the baseline PLC value to account for native embolisms, the Ψ_{stem} inducing 50% of PLC (P50) was not statistically different between two estimates from this study (unadjusted EC50: -1.6 MPa, grey line; and recalculated PLC: -1.58 MPa, Fig. 2a blue line) and P50 (-1.75 MPa; Fig. 2a red circles) reported in the previous study (Secchi & Zwieniecki, 2014).

To facilitate current and future analysis of X-ray micro-CT scans for estimation of embolism extent, we tested the correlation between calculated PLC, determined from the diameters of all vessels (see material and methods) with simple measurements of the total area of embolized vessels (AEV), to total area of mature xylem (AMX; Fig. 3 inset). The correlation was

linear with $R^2=0.97$ ($N=14$, $p<0.0001$) allowing for simplified analysis of embolism formation (Fig. 1S). Changes in embolism extent using the AEV/AMX ratio ranged from ~ 0 in non-stressed plants to $7.72\% \pm 1.35$ in stressed poplars, with a ψ_{stem} of -2.32 ± 0.21 MPa, and an EC50 of ~ -1.92 MPa (we used EC50 to describe a 50% change over the range of observed values, not a true change in conductivity) when fitted with a four-parameter logistic curve (black circles, Fig. 3a). Embolism extent in plants that underwent water-stress treatments to levels below -2.0 MPa, and were subsequently re-watered and allowed to recover for several hours ($\psi_{\text{stem}} -0.93 \pm 0.18$ MPa) was $2.92\% \pm 0.14$, significantly lower than the extent determined for stressed plants that did not recover ($p<0.0001$; Fig. 3a). This reduction in the AEV:AMX ratio suggests that plants recovering from water stress have fewer embolised xylem conduits than they did before re-watering. The formation of embolisms and their disappearance followed a specific spatial pattern, with embolism formation beginning near the pith and extending toward the cambium (i.e. inside-out). This was confirmed by analysis of the ratio between distance of the closest embolized vessel to cambium (EV-to-C) in each ray parenchyma wedge to distance between pith and cambium (P-to-C; Fig. 4, black circles). In plants recovering from stress, we observed a significant increase of the average ratio (EV-to-C:P-to-C), suggesting that refilling of vessels occurred in opposite direction, with regions that embolized last, recovering first (outside-in; Fig. 4, white circles).

We used three independent approaches to experimentally manipulate the chemistry of xylem sap (pH and content of soluble sugars in sap) during the recovery process. Our first approach changed xylem sap pH by infiltrating stems with a pH buffer (pH 6.5), reducing the activity of acidic invertases. Secondly, we reduced membrane ATP-ase transport capacity by infiltrating stems with sodium orthovanadate (NaVO_3) solution to disable sucrose transporters. Our third approach was to reduce respiration by infiltrating stems with sodium cyanide (NaCN) solution and exposing plants to gaseous carbon monoxide (CO) to reduce the availability of ATP. As a control we infiltrated stems with DI water. In all cases, and independent of the treatments, plants were capable of recovering water potential to non-stress levels within 24 hours of re-watering (Fig. 5a). Only NaVO_3 and CO treatments were effective in significantly increasing xylem sap pH to ~ 6.6 , while the control stress-were at pH ~ 5.9 and water infiltration at pH ~ 6.2 (ANOVA one-way $p=0.001$; Fig. 5b). Treatments with a pH buffer or NaCN did not

result in significant changes of xylem sap pH, either due to their short-term effects or the plant's capacity to overcome their presence. High pH values (NaVO₃, CO) resulted in low sugar concentrations, while all remaining treatments and stressed plants that had low xylem sap pH had a higher sugar content (Fig. 5b inset).

We selected the NaVO₃ treatment, for its significant impact on pH and the simplicity of its *in vivo* application, to determine the impact of metabolic activity on hydraulic recovery, as determined by presence of embolized vessels. Following the timeline established through our greenhouse experiment, NaVO₃ solution was allowed to infiltrate the stems of non-stressed and severely-stressed plants (< -2.0 MPa). Subsets of each group were scanned using X-ray micro-CT. Remaining stressed plants were re-watered and allowed adequate time for rehydration (from 4 to 24 hours) before scanning. Each plant was scanned only once to avoid X-ray exposure induced tissue damage. We did not find any impact of NaVO₃ infiltration on the AEV/AMX ratio in non-stressed plants, suggesting that treatment with NaVO₃ had no effect on xylem native embolism (AEV/AMX ratio = ~0.0068; Fig. 6). Similarly, there was no difference on embolism extent between severely stressed non-treated, and NaVO₃-treated plants (AEV/AMX ratio = respectively 0.072 ± 0.016 and 0.067 ± 0.024 ; Fig. 6). However, we found a significant effect on AEV/AMX ratio between NaVO₃ treated and non-treated plants after several hours of plant rehydration, with treated plants showing small non-significant level of recovery (AEV/AMX ratio change from 0.067 ± 0.024 to 0.0534 ± 0.023 ; Fig. 6), while non-treated plants showed substantial recovery of more than 50% of their conductive capacity (AEV/AMX ratio change from 0.072 ± 0.016 to 0.029 ± 0.013 ; Fig. 6), there was no difference in recovery of stem water potential (Fig. 6).

Discussion

Combining experimental manipulations of xylem physiochemical status and X-ray micro-CT observations of living plants, we show that treatments resulting in high apoplastic pH during water stress are detrimental to the accumulation of soluble sugars in xylem, significantly reducing the capacity of trees to refill embolized vessels upon recovery from stress without impacting the recovery of stem water potential. Our results verify that recovery of water potential is a non-metabolic process, while reinforcing the idea that embolism refilling – even

under without water stress – requires biological activity of VACs. Direct observations of xylem vessels during recovery from water stress in a high pH environment support our hypothesis that restoration of xylem transport capacity requires chemical priming. The chemical priming of xylem involves both drop in sap pH and the accumulation of sugars in non-functional vessels (Secchi & Zwieniecki, 2012).

In this study, X-ray micro-CT observations were used to determine both the embolism formation during the plant dehydration and the hydraulic recovery following trees re-watering. These *in vivo* observations confirmed that, when low tension was restored, previously droughted poplar plants recovered from stress by reducing the number of embolized vessels, and potentially reducing PLC. After 4 to 24 hours poplars repair ~ 60% of previously embolized conduits. The results of this partial refilling presented here are consistent with xylem hydraulic recovery measured previously on poplars belonging to the same clone, showing that full restoration of stem hydraulic capacity can take several days (Secchi & Zwieniecki, 2014; Pagliarani *et al.*, 2019). Two-dimensional analyses of X-ray micro-CT scans provided detailed information on the propagation of xylem embolism during dehydration and recovery after irrigation. Initially, embolism occurred in the primary xylem adjacent to the pith before spreading toward the cambium in correlation with increasing tension. Similar results were reported for *Populus tremula x alba* clone (Choat *et al.*, 2016) and for *Vitis vinifera* (Brodersen *et al.*, 2013), where embolisms also form first in the vessels surrounding the pith, and with the increasing stress, spread radially toward the cambium within sectors of grouped vessels, via inter-vessel connections and conductive xylem relays (Brodersen *et al.*, 2013). These previous results show that older vessels are more prone to low-tension embolism formation, potentially suggesting the presence of some degenerative processes that can limit the length of time that vessels can function under excessive tension. It could also be possible that older vessels are more susceptible to embolism due to cavitation fatigue (Hacke *et al.*, 2001; Stiller and Sperry, 2002), although in our experiment we did not allow plants to get stress prior to experiment. Radial embolism propagation, bounded by presence of parenchyma rays, may reflect the occurrence of air seeding from interior vessels toward the outer perimeter, along the path of greatest vessel-to-vessel contact (Choat *et al.*, 2008).

While the spread of embolism is relatively well documented, much less is known about

the spatial dynamics of vessel refilling. We observed recovery of embolized conduits in the opposite direction to their propagation, i.e. outside-in, from the cambium toward the pith. Although we did not observe full recovery, the extent of refilling was consistent with expected values given the post-stress stem water potential. In multiple cases, recovery resulted in a decrease of the average distance between the furthest embolized vessel and the pith, thus suggesting that proximity to cambium is important in providing resources (sugars, ATP and potentially water) for filling embolized vessels. Numerous studies have shown that non-structural sugars are crucial for maintenance of xylem hydraulic function under water stress (Trifilo *et al.*, 2017; Tomasella *et al.*, 2019b; Tomasella *et al.*, 2020), and especially for recovery of the hydraulic capacity of the xylem after drought relief (Secchi & Zwieniecki, 2011; Pagliarani *et al.*, 2019; Tomasella *et al.*, 2019a). Theoretical models of embolism removal try to resolve the energy need (Nardini *et al.*, 2011; Secchi & Zwieniecki, 2016; Pagliarani *et al.*, 2019), by proposing that, during water stress, osmotica accumulate in the apoplast in the form of sugars and ions. Direct analysis of xylem sap in embolized vessels indeed supports this view, as both sugars and ions accumulated in non-functional vessels can provide an adequate osmotic potential gradient to drain water from parenchyma cells post-recovery (Secchi & Zwieniecki, 2012). Sugars, mostly sucrose derived from starch degradation, are moved from symplast to apoplast through the membrane (passively) or by a proton-coupled sucrose efflux (actively). The accumulation of sugars is controlled by xylem pH, which drops during water stress. A lower pH induces apoplastic sucrose hydrolysis, possibly through acidic invertase activity (Pagliarani *et al.*, 2019), and shifts the sucrose concentration gradient thereby establishing a further efflux of sucrose to apoplast. The resulting accumulation of sugar decreases apoplastic water potential, pulling water into the empty vessels upon relief from drought (Salleo *et al.*, 2009; Zwieniecki & Holbrook, 2009; Secchi & Zwieniecki, 2012; Secchi & Zwieniecki, 2016). Proton-coupled sucrose efflux is predicted by models to be responsible for the initial increase of apoplastic sucrose concentration and the decrease in pH, seen in poplar. The consequent drop in pH, triggers an ion efflux from living cells that additionally contributes to apoplastic osmotic concentration (Secchi & Zwieniecki, 2011; Secchi & Zwieniecki, 2012). The source of ions might be related to proximity to cambium and phloem, which would be required for recycling of potassium ions to maintain the capacity for this activity (Thompson/Holbrook/Zwieniecki),

407 further explaining the pattern of refilling from the outside-in.

408 *In vitro*, it has been shown that in a low-pH environment, sugars continuously
409 accumulate in the xylem apoplast, and that this carbohydrate accumulation is significantly
410 reduced in the presence of vanadate, a proton pump blocker (Secchi & Zwieniecki, 2011;
411 Secchi & Zwieniecki, 2012; Secchi & Zwieniecki, 2016). Here, we prove that, when the
412 metabolic activity of stems is decreased, the extent of recovery during rehydration is
413 significantly reduced (Fig. 6). Stem infiltration with vanadate impeded the removal of
414 embolisms formed during drought (only 20% of embolized vessels recovered after stress relief),
415 while a greater extent of embolism removal (about 60%) was observed in water-treated plants.
416 Similar results were obtained in *Laurus nobilis* L., where stems radially supplied with vanadate
417 did not recover from PLC after 20 min of rehydration to low tension (Salleo *et al.*, 2004). Here
418 we provided a relatively longer water stress relief period (4 to 24 hours), and natural light
419 conditions that encompassed night. Despite this prolonged time and a period of no transpiration,
420 embolized vessels remained non-functional when metabolic activity had been reduced with
421 vanadate. This lack of recovery is associated with high xylem pH (>6) and lower soluble sugar
422 content in xylem sap (Fig. 5), suggesting that in the absence of metabolic activity, there was no
423 priming of the stem for recovery, directly linking plant chemistry to visual observations of
424 refilling activity.

425 The vulnerability curve generated by the X ray micro-CT observations did not closely
426 match the curve based on the classical hydraulic techniques, previously performed on plants
427 belonging to the same poplar clone (Secchi & Zwieniecki, 2014). The *in vivo* observations
428 resulted in underestimation of embolism formation with a maximum of PLC around 50%. The
429 discrepancy in PLC values obtained with the two techniques could be attributed to two factors.
430 First X-ray micro-CT analyses are based on transverse bidimensional reconstructed images of a
431 small scanned segment of stems, and therefore image analysis may miss partially embolized
432 vessels, and could thereby overestimate maximum conductance (Loepfe *et al.*, 2007; Pratt &
433 Jacobsen, 2018). These nonfunctional vessels, are however, accounted for in the hydraulic
434 measurements that typically examine much longer stem segments. Conversely, it is possible that
435 these traditional measurements overestimate the conductive tissue in studied stems, as the outer
436 most layer of xylem may not, as here, show any symptoms of embolisms. The outermost xylem

section was also slightly higher in average pixel brightness (i.e., more dense) suggesting greater hydration of this part of the stem and possibility that, despite visible vessels, the near-cambial sector may be immature and not yet substantially contribute to axial transport. Underestimation of embolism level, through X-ray micro-CT analysis, was observed before in *Q. robur* plants (Choat *et al.*, 2016); the authors suggested the possibility that many of the cells that appeared filled in the images were still living and therefore non functional in transporting water. Pratt and Jacobsen (2018) reported that in grapevine and American chestnut, some vessels commonly observed in the outer growth rings were not contributing to transpiration, and when the samples were dehydrated with air, these vessels showed some deformation suggesting that they were not yet fully lignified (Pratt & Jacobsen, 2018). In our case, the evidence that vessels located in the outer layer of xylem were not involved in water transport (or were not experiencing tension) were obtained experimentally by rescanning stem segments that were cut in the air few mm below the scanned area and allowed to form embolism due to suction in functional vessels. No vessels in the outer layer ever were found to form embolisms. When only mature vessels (the ones that formed embolisms after cutting in the air) were used in the calculation of PLC, the resulting PLC was almost identical to previous data obtained from hydraulic measurements (Fig 2a).

Our results confirm that poplar trees, after re-watering and under low tension, can recover from water stress by reducing the number of embolized vessels in their stems. Further, we show that refilling is an active, energy-dependent process that relies on metabolically-driven acidification to accumulate sugars in the apoplast during water stress. By comparing *in vivo* images (without rescanning that could damage VACs) from two groups of water-stressed plants – with and without experimentally reduced metabolic activity – we can conclude that refilling is a part of the life of trees, and requires further studies to fully understand how it limits stress survival.

Acknowledgements

This study was made possible by Elettra Sincrotrone Trieste, which granted access to the SYRMEP beamline (proposal no: 20165201). We thank the technical staff at SYRMEP for the assistance during experiments. Francesca Secchi gratefully acknowledges funding from Ateneo

CSP/2016 Project (University of Turin). The authors wish to thank Tiziano Strano for poplar maintenance and Alana Chin for critical reading and help with English editing of the manuscript.

Author Contribution

FS and MAZ planned and designed the research. FS, CP and MAZ performed the chemical experiments in Turin. FS, CP, SC, FP, TS, GT, AN and MAZ were involved in micro CT observations. FS, SC, GT, FP made the image reconstruction. FS, CP, SC, FP, GT, MMO, CL, AN and MAZ contributed to the analysis and discussion of data. FS, MAZ and AN wrote the manuscript, with contribution and revision from all other authors.

References

- Brodersen CR, Knipfer T, McElrone AJ. 2018.** In vivo visualization of the final stages of xylem vessel refilling in grapevine (*Vitis vinifera*) stems. *New Phytologist* **217**(1): 117-126.
- Brodersen CR, McElrone AJ. 2013.** Maintenance of xylem network transport capacity: a review of embolism repair in vascular plants. *Frontiers in Plant Science* **4**.
- Brodersen CR, McElrone AJ, Choat B, Lee EF, Shackel KA, Matthews MA. 2013.** In Vivo Visualizations of Drought-Induced Embolism Spread in *Vitis vinifera*. *Plant Physiology* **161**(4): 1820-1829.
- Brodersen CR, McElrone AJ, Choat B, Matthews MA, Shackel KA. 2010.** The Dynamics of Embolism Repair in Xylem: In Vivo Visualizations Using High-Resolution Computed Tomography. *Plant Physiology* **154**(3): 1088-1095.
- Brun F, Pacile S, Accardo A, Kourousias G, Dreossi D, Mancini L, Tromba G, Pugliese R. 2015.** Enhanced and Flexible Software Tools for X-ray Computed Tomography at the Italian Synchrotron Radiation Facility Elettra. *Fundamenta Informaticae* **141**(2-3): 233-243.
- Charrier G, Torres-Ruiz JM, Badel E, Burlett R, Choat B, Cochard H, Delmas CEL, Domec JC, Jansen S, King A, et al. 2016.** Evidence for Hydraulic Vulnerability

Segmentation and Lack of Xylem Refilling under Tension. *Plant Physiology* **172**(3): 1657-1668.

Choat B, Badel E, Burlett R, Delzon S, Cochard H, Jansen S. 2016. Noninvasive Measurement of Vulnerability to Drought-Induced Embolism by X-Ray Microtomography. *Plant Physiology* **170**(1): 273-282.

Choat B, Cobb AR, Jansen S. 2008. Structure and function of bordered pits: new discoveries and impacts on whole-plant hydraulic function. *New Phytologist* **177**(3): 608-625.

Choat B, Nolf M, Lopez R, Peters JMR, Carins-Murphy MR, Creek D, Brodribb TJ. 2019. Non-invasive imaging shows no evidence of embolism repair after drought in tree species of two genera. *Tree Physiology* **39**(1): 113-121.

Clearwater M, Goldstein G 2005. Embolism repair and long distance transport. In: Holbrook NM, Zwieniecki MA eds. *Vascular Transport in Plants*: Elsevier, 201-220.

Cochard H, Badel E, Herbette S, Delzon S, Choat B, Jansen S. 2013. Methods for measuring plant vulnerability to cavitation: a critical review. *Journal of Experimental Botany* **64**(15): 4779-4791.

Cochard H, Delzon S, Badel E. 2015. X-ray microtomography (micro-CT): a reference technology for high-resolution quantification of xylem embolism in trees. *Plant Cell and Environment* **38**(1): 201-206.

Fukuda K, Kawaguchi D, Aihara T, Ogasa MY, Miki NH, Haishi T, Umebayashi T. 2015. Vulnerability to cavitation differs between current-year and older xylem: non-destructive observation with a compact magnetic resonance imaging system of two deciduous diffuse-porous species. *Plant Cell and Environment* **38**(12): 2508-2518.

Holbrook NM, Ahrens ET, Burns MJ, Zwieniecki MA. 2001. In vivo observation of cavitation and embolism repair using magnetic resonance imaging. *Plant Physiology* **126**(1): 27-31.

Jensen KH, Berg-Sorensen K, Bruus H, Holbrook NM, Liesche J, Schulz A, Zwieniecki MA, Bohr T. 2016. Sap flow and sugar transport in plants. *Reviews of Modern Physics* **88**(3).

524 **Knipfer T, Cuneo IF, Brodersen CR, McElrone AJ. 2016.** In Situ Visualization of the
525 Dynamics in Xylem Embolism Formation and Removal in the Absence of Root Pressure:
526 A Study on Excised Grapevine Stems. *Plant Physiology* **171**(2): 1024-1036.

527 **Lamarque LJ, Corso D, Torres-Ruiz JM, Badel E, Brodribb TJ, Burlett R, Charrier G,**
528 **Choat B, Cochard H, Gambetta GA, et al. 2018.** An inconvenient truth about xylem
529 resistance to embolism in the model species for refilling *Laurus nobilis* L. *Annals of*
530 *Forest Science* **75**(3).

531 **Leyva A, Quintana A, Sanchez M, Rodriguez EN, Cremata J, Sanchez JC. 2008.** Rapid and
532 sensitive anthrone-sulfuric acid assay in microplate format to quantify carbohydrate in
533 biopharmaceutical products: Method development and validation. *Biologicals* **36**(2): 134-
534 141.

535 **Loepfe L, Martinez-Vilalta J, Pinol J, Mencuccini M. 2007.** The relevance of xylem network
536 structure for plant hydraulic efficiency and safety. *Journal of Theoretical Biology* **247**(4):
537 788-803.

538 **McElrone AJ, Choat B, Parkinson DY, MacDowell AA, Brodersen CR. 2013.** Using High
539 Resolution Computed Tomography to Visualize the Three Dimensional Structure and
540 Function of Plant Vasculature. *Jove-Journal of Visualized Experiments*(74).

541 **Nardini A, Lo Gullo MA, Salleo S. 2011.** Refilling embolized xylem conduits: Is it a matter of
542 phloem unloading? *Plant Science* **180**(4): 604-611.

543 **Nardini A, Savi T, Losso A, Petit G, Pacile S, Tromba G, Mayr S, Trifilo P, Lo Gullo MA,**
544 **Salleo S. 2017.** X-ray microtomography observations of xylem embolism in stems of
545 *Laurus nobilis* are consistent with hydraulic measurements of percentage loss of
546 conductance. *New Phytologist* **213**(3): 1068-1075.

547 **Nolf M, Lopez R, Peters JMR, Flavel RJ, Kolodzin LS, Young IM, Choat B. 2017.**
548 Visualization of xylem embolism by X-ray microtomography: a direct test against
549 hydraulic measurements. *New Phytologist* **214**(2): 890-898.

550 **Ogasa MY, Utsumi Y, Miki NH, Yazaki K, Fukuda K. 2016.** Cutting stems before relaxing
551 xylem tension induces artefacts in *Vitis coignetiae*, as evidenced by magnetic resonance
552 imaging. *Plant Cell and Environment* **39**(2): 329-337.

553 **Pagliarani C, Casolo V, Beiragi MA, Cavalletto S, Siciliano I, Schubert A, Gullino ML,**
 554 **Zwieniecki MA, Secchi F. 2019.** Priming xylem for stress recovery depends on
 555 coordinated activity of sugar metabolic pathways and changes in xylem sap pH. *Plant*
 556 *Cell and Environment* **42**(6): 1775-1787.

557 **Petruzzellis F, Pagliarani C, Savi T, Losso A, Cavalletto S, Tromba G, Dullin C, Bar A,**
 558 **Ganthaler A, Miotto A, et al. 2018.** The pitfalls of in vivo imaging techniques: evidence
 559 for cellular damage caused by synchrotron X-ray computed micro-tomography. *New*
 560 *Phytologist* **220**(1): 104-110.

561 **Pratt RB, Jacobsen AL. 2018.** Identifying which conduits are moving water in woody plants: a
 562 new HRCT-based method. *Tree Physiology* **38**(8): 1200-1212.

563 **Rolland V, Bergstrom DM, Lenne T, Bryant G, Chen H, Wolfe J, Holbrook NM, Stanton**
 564 **DE, Ball MC. 2015.** Easy Come, Easy Go: Capillary Forces Enable Rapid Refilling of
 565 Embolized Primary Xylem Vessels. *Plant Physiology* **168**(4): 1636-1647.

566 **Salleo S, Lo Gullo MA, Trifilo' P, Nardini A. 2004.** New evidence for a role of vessel-
 567 associated cells and phloem in the rapid xylem refilling of cavitated stems of *Laurus*
 568 *nobilis* L. *Plant, Cell and Environment* **27**: 1065-1076.

569 **Salleo S, Trifilo' P, Esposito S, Nardini A, Lo Gullo MA. 2009.** Starch-to-sugar conversion in
 570 wood parenchyma of field-growing *Laurus nobilis* plants: a component of the signal
 571 pathway for embolism repair? *Functional Plant Biology* **36**: 815-825.

572 **Savi T, Miotto A, Petruzzellis F, Losso A, Pacile S, Tromba G, Mayr S, Nardini A. 2017.**
 573 Drought-induced embolism in stems of sunflower: A comparison of in vivo micro-CT
 574 observations and destructive hydraulic measurements. *Plant Physiology and*
 575 *Biochemistry* **120**: 24-29.

576 **Scheenen TWJ, Vergeldt FJ, Heemskerk AM, Van As H. 2007.** Intact plant magnetic
 577 resonance imaging to study dynamics in long-distance sap flow and flow-conducting
 578 surface area. *Plant Physiology* **144**(2): 1157-1165.

579 **Scoffoni C, Sack L. 2015.** Are leaves 'freewheelin'? Testing for a Wheeler-type effect in leaf
 580 xylem hydraulic decline. *Plant Cell and Environment* **38**(3): 534-543.

581 **Secchi F, Zwieniecki MA. 2011.** Sensing embolism in xylem vessels: the role of sucrose as a
 582 trigger for refilling. *Plant, Cell and Environment* **34**(3): 514-524.

- Secchi F, Zwieniecki MA. 2012.** Analysis of Xylem Sap from Functional (Nonembolized) and Nonfunctional (Embolized) Vessels of *Populus nigra*: Chemistry of Refilling. *Plant Physiology* **160**(2): 955-964.
- Secchi F, Zwieniecki MA. 2014.** Down-Regulation of Plasma Intrinsic Protein1 Aquaporin in Poplar Trees Is Detrimental to Recovery from Embolism. *Plant Physiology* **164**(4): 1789-1799.
- Secchi F, Zwieniecki MA. 2016.** Accumulation of sugars in the xylem apoplast observed under water stress conditions is controlled by xylem pH. *Plant Cell and Environment* **39**(11): 2350-2360.
- Stroock AD, Pagay VV, Zwieniecki MA, Holbrook NM 2014.** The Physicochemical Hydrodynamics of Vascular Plants. In: Davis SH, Moin P eds. *Annual Review of Fluid Mechanics, Vol 46*, 615-642.
- Tomasella M, Casolo V, Aichner N, Petruzzellis F, Savi T, Trifilo P, Nardini A. 2019a.** Non-structural carbohydrate and hydraulic dynamics during drought and recovery in *Fraxinus ornus* and *Ostrya carpinifolia* saplings. *Plant Physiology and Biochemistry* **145**: 1-9.
- Tomasella M, Nardini A, Hesse BD, Machlet A, Matyssek R, Haberle KH. 2019b.** Close to the edge: effects of repeated severe drought on stem hydraulics and non-structural carbohydrates in European beech saplings. *Tree Physiology* **39**(5): 717-728.
- Tomasella M, Petrusa E, Petruzzellis F, Nardini A, Casolo V. 2020.** The Possible Role of Non-Structural Carbohydrates in the Regulation of Tree Hydraulics. *International Journal of Molecular Sciences* **21**(1).
- Trifilo P, Casolo V, Raimondo F, Petrusa E, Boscutti F, Lo Gullo MA, Nardini A. 2017.** Effects of prolonged drought on stem non-structural carbohydrates content and post-drought hydraulic recovery in *Laurus nobilis* L.: The possible link between carbon starvation and hydraulic failure. *Plant Physiology and Biochemistry* **120**: 232-241.
- Trifilo P, Raimondo F, Lo Gullo MA, Barbera PM, Salleo S, Nardini A. 2014.** Relax and refill: xylem rehydration prior to hydraulic measurements favours embolism repair in stems and generates artificially low PLC values. *Plant Cell and Environment* **37**(11): 2491-2499.

- 612 **Tyree MT, Zimmermann MH. 2002.** *Xylem Structure and the Ascent of Sap*. New York:
613 Springer-Verlag.
- 614 **Wang MT, Tyree MT, Wasylishen RE. 2013.** Magnetic resonance imaging of water ascent in
615 embolized xylem vessels of grapevine stem segments. *Canadian Journal of Plant Science*
616 **93(5): 879-893.**
- 617 **Wheeler JK, Huggett BA, Tofte AN, Rockwell FE, Holbrook NM. 2013.** Cutting xylem under
618 tension or supersaturated with gas can generate PLC and the appearance of rapid
619 recovery from embolism. *Plant Cell and Environment* **36(11): 1938-1949.**
- 620 **Zwieniecki MA, Holbrook NM. 2009.** Confronting Maxwell's demon: biophysics of xylem
621 embolism repair. *Trends in Plant Science* **14(10): 530-534.**
- 622 **Zwieniecki MA, Melcher PJ, Ahrens ET. 2013.** Analysis of spatial and temporal dynamics of
623 xylem refilling in *Acer rubrum* L. using magnetic resonance imaging. *Frontiers Plant*
624 *Science* **4: 265.**

Figure legends

Fig. 1 (a) Schematic representation of experimental set-up. (b) Stem infiltration with sodium ortho-vanadate solution. (c) Plant exposure to carbon monoxide.

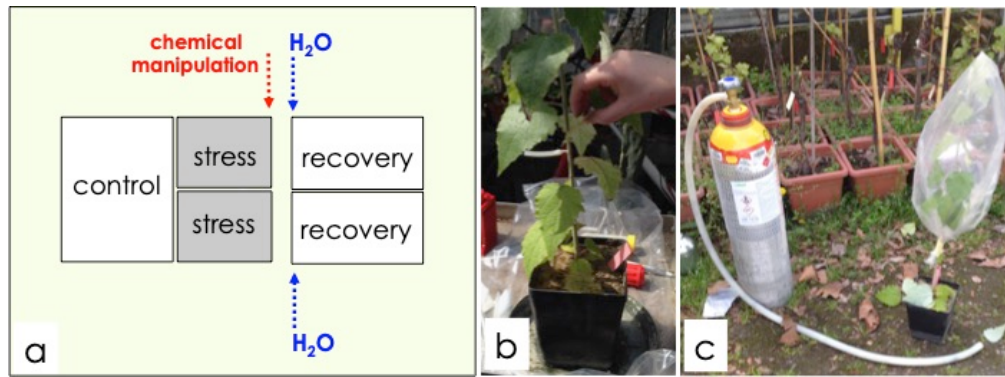
Fig. 2 (a) Vulnerability curves for *Populus alba x tremula* plants based on: xylem theoretical hydraulic conductivity of plants subjected to one x-ray exposure (grey circles-lines); xylem theoretical hydraulic conductivity normalized with data obtained by stems first air-cut (to induce maximum artificial embolism formation) and then re-scanned (black circles and blue lines); hydraulic measurements previously performed on the same poplar clone (red circles, Secchi and Zwieniecki 2014). Each circle corresponds to a plant. (b) *In vivo* visualization by X-ray microtomography of xylem emboli in stems of *Populus tremula x alba* intact plants. Reconstructed cross sections showing gas-filled (dark grey) and water-filled (light grey) xylem conduits during well watered and stress conditions. 1-2 cross-sections of stressed and control stems scanned once and the same stems exposed to a second exposure after air-cutting (3-4).

Fig. 3 (a) Percent of total area of embolized vessels (AEV) on total area of mature xylem (AMX) in response to changes in xylem pressure during drought and recovery treatments. Data were fitted with a four-parameter logistic curve (dose-response curve); each circle corresponds to a plant. (b) *In vivo* visualization by X-ray microtomography (micro-CT) in stems of intact *Populus tremula x alba* plants. Reconstructed cross-sections showing embolized (air-filled vessels, dark circles) and functional conduits (water-filled, light grey circles) in stressed, recovered, and well-watered plants, respectively.

Fig. 4 Ratio between the distance of the closest embolized vessels to cambium (EV-to-C) in each ray parenchyma wedge to the distance between the pith and cambium (P-to-C) in stressed, well-watered, and recovered plants. Circles are mean values of multiple embolized vessels belonging to a single plant and error bars represent SD. Inset: Reconstructed cross section showing distance from pith to the cambium (yellow lines) and from the closest embolized vessels to cambium (red dotted lines).

Fig. 5 Effect of chemical treatments (sodium orthovanadate, NaVO_3 ; carbon monoxide, CO ; pH6.5 buffer solution and sodium cyanide, NaCN) on: (a) Xylem pressure measured on non-transpiring leaves (Ψ_{stem}). and (b) xylem pH. Inset: average xylem sugar content measured for each treatment as it relates to average pH values. All plants were water-stressed and then chemically treated, allowing for 1 day for acclimation. Poplars were re-watered, and after 24 hours of recovery, xylem sap was collected. One-way ANOVA test suggests significant differences in xylem pressure ($p < 0.001$), pH values ($p = 0.001$) and sugar content ($p < 0.001$) between different chemical treatments in plants recovering from stress. Letters denote homogeneous groups based on the Fisher LSD method; bars are mean values, and error bars represent SE.

Fig. 6 Percentage of total area of embolized vessels (AEV) on total area of mature xylem (AMX) in response to xylem pressure for non treated plants (black circles) and for poplar that before the recovery phase were chemical treated with a solution 10 mM of sodium orthovanadate (light grey squares). Symbols are mean values of multiple embolized vessels belonging to a single plant and error bars represent SD. Asterisk denotes significant differences between treated and non-treated, recovering plants, tested using a t-test ($p < 0.05$).



676

677 Fig. 1

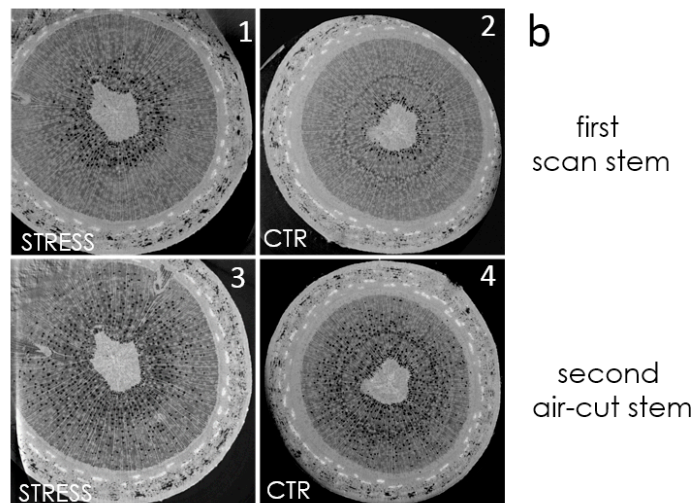
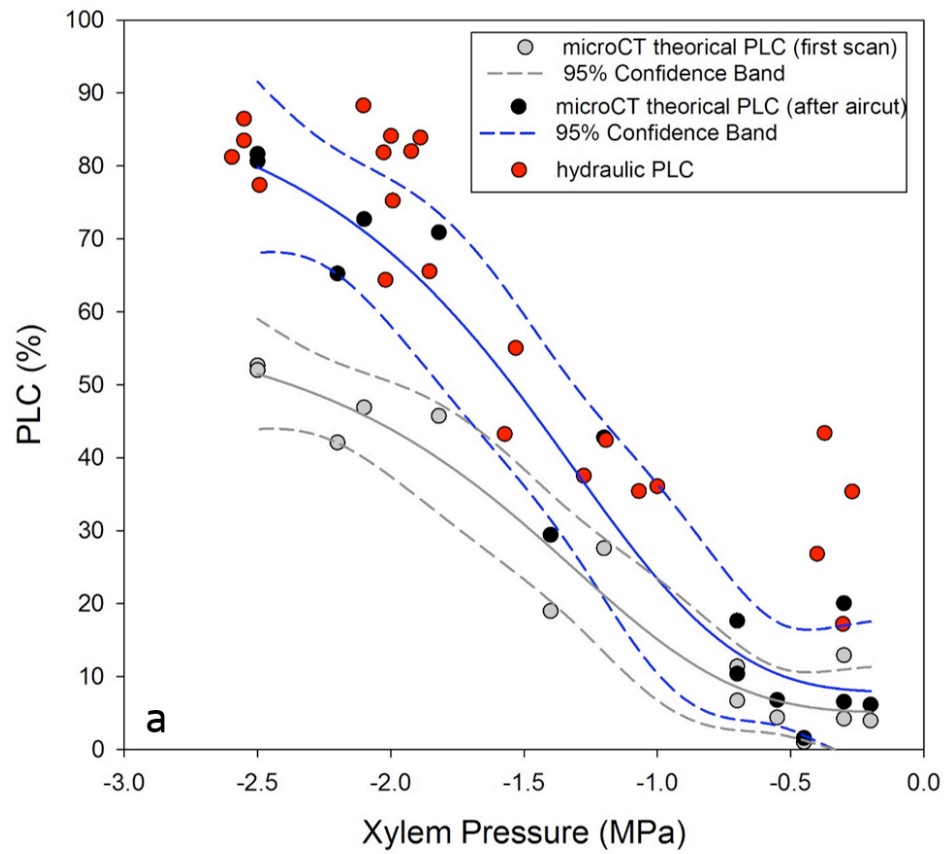


Fig. 2

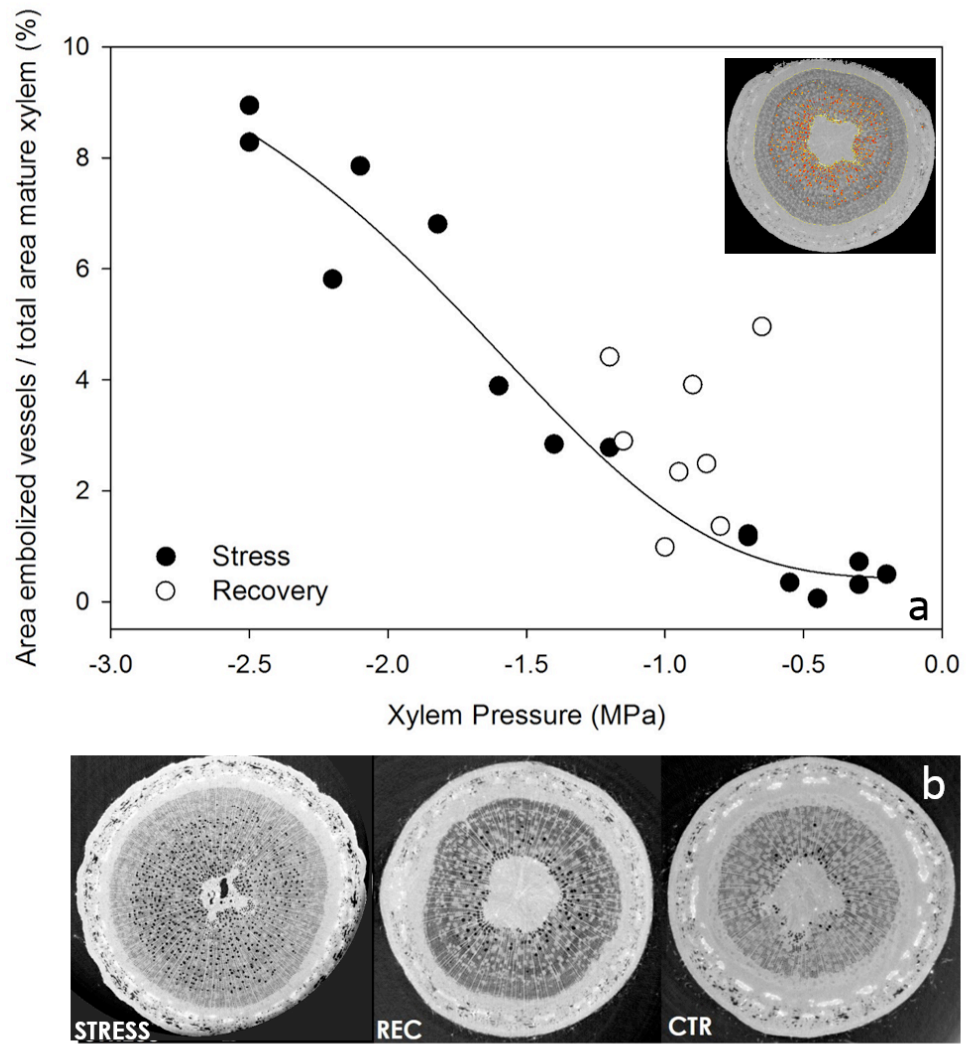
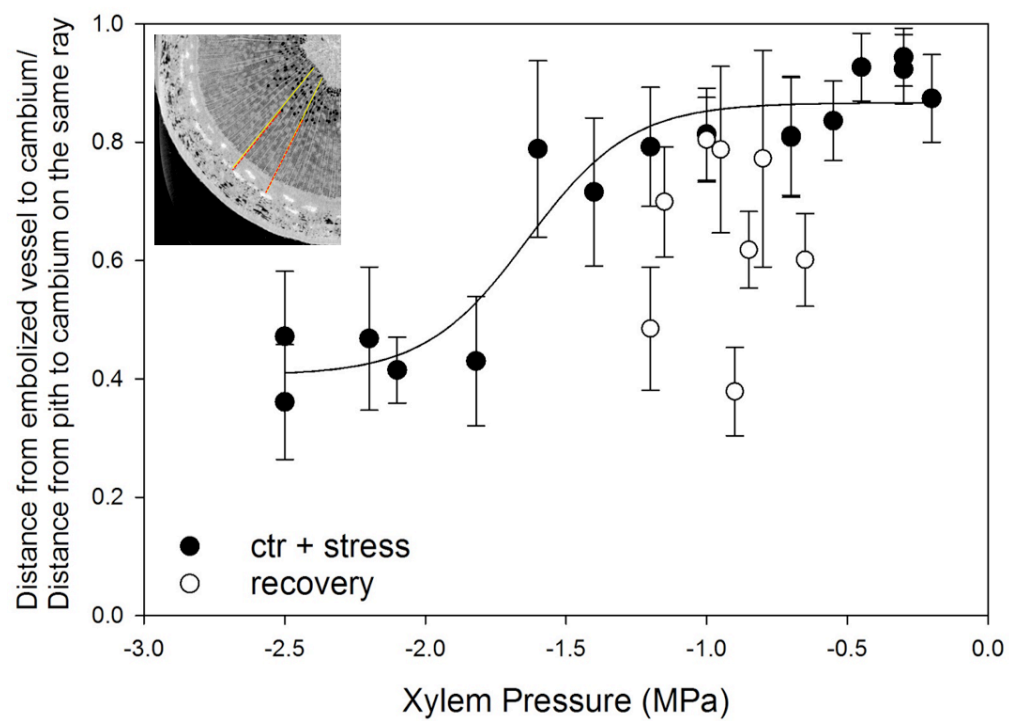


Fig. 3



686

687 Fig. 4

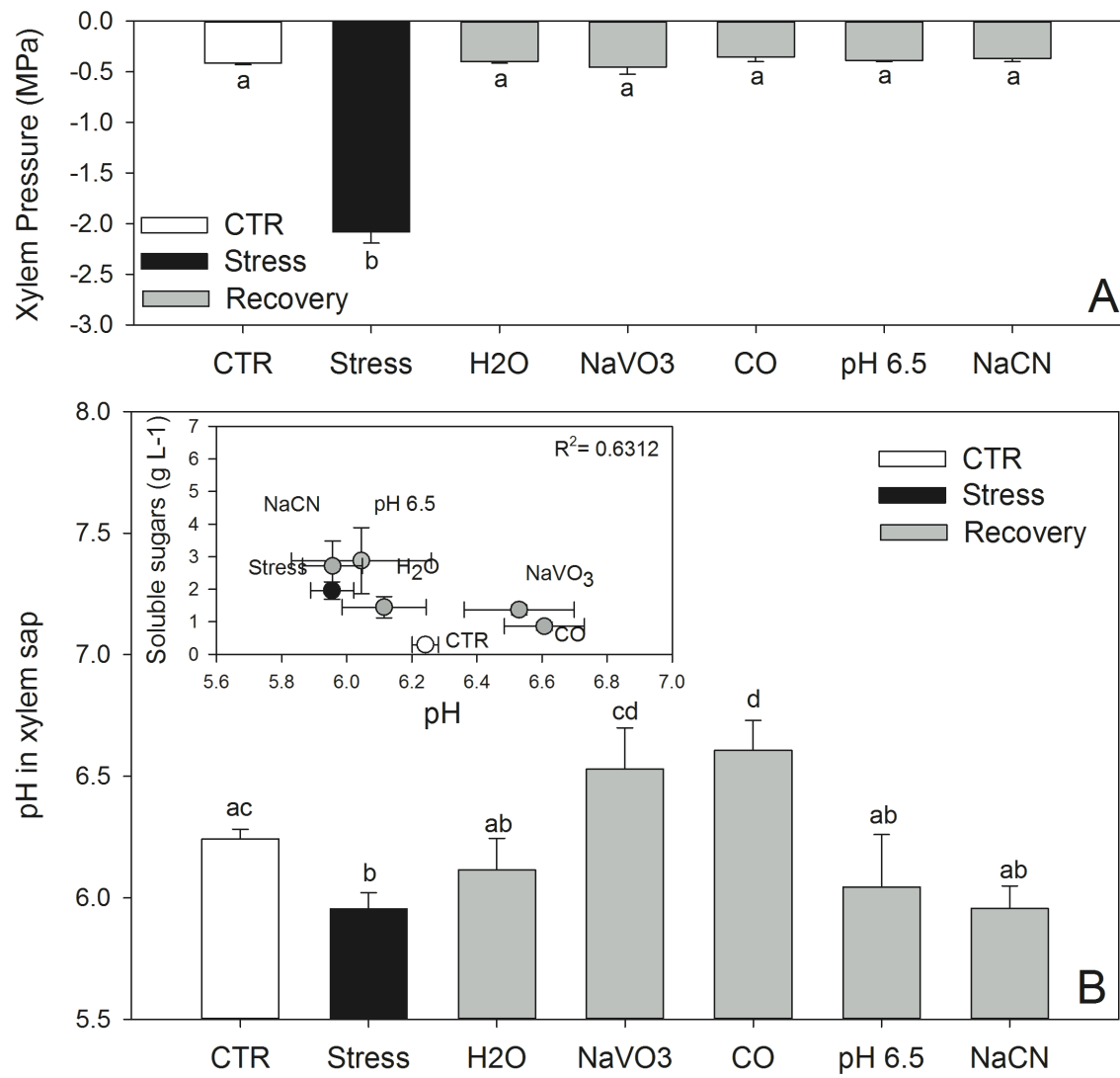


Fig. 5

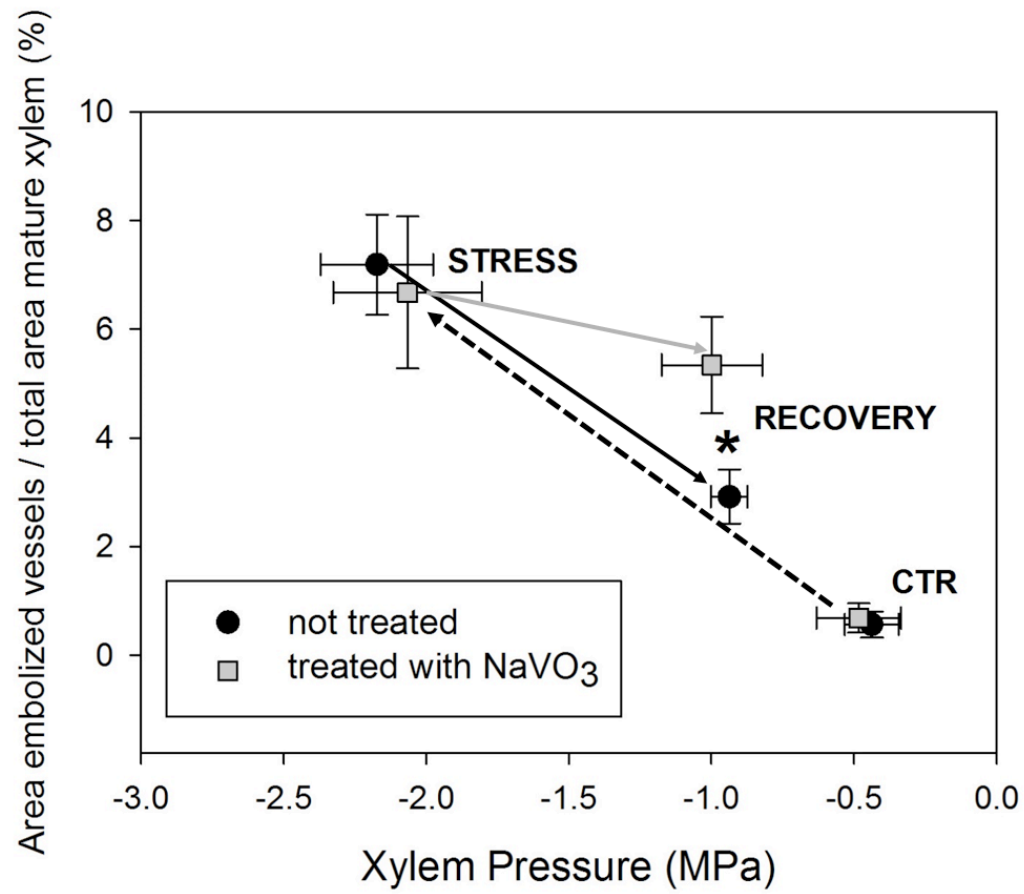


Fig. 6